27th EPS Conference on Contr. Fusion and Plasma Phys. Budapest, 12-16 June 2000 ECA Vol. **24B** (2000) 536 -539

Cause of mode-locking phenomena in TPE-RX

H. Koguchi, Y. Yagi, J-A. Malmberg[1], Y. Hirano, T. Shimada,
S. Sekine and H. Sakakita

Electrotechnical Laboratory, M. I. T. I., 1-1-4 Umezono, Tsukuba, Ibaraki, 305-8568 Japan

[1] *Royal Institute of Technology, S-10044 Stockholm, Sweden*

1.Introduction

We present a discussion on the cause of the locked mode in TPE-RX. The locked modes have been observed in many reversed field pinch (RFP) plasmas. Phase of several dynamo modes lock at a certain location, and form a toroidally localized magnetic perturbation (called slinky mode). In MST, the slinky modes rotate during the sawtooth events, and lock to the field error generated by the sawtooth crash at the poloidal shell gap [1]. In RFX, the locked mode appears in 100 % of the discharges. The slinky mode locks to the wall just after the RFP formation [2]. The locked mode gives rise to a serious wall loading problem, and limits the plasma current. In TPE-RX, the locked mode is also found to exist, and disappears under certain experimental conditions (e.g. low filling pressure of the fueling gas) [3]. Two hypotheses for the locked mode to occur in RFP plasma have been considered. The first one is the existence of the halo current [3], and the second one is the braking effect of the electromagnetic torque due to the eddy current induced in the vacuum vessel by the rotating dynamo modes [4]. We measured the toroidal distribution of the vessel current, and the current signal at the locked position is observed. We also show the mode rotation, and the mode spectrum.

2. Vessel current measurement

Figure 1 shows an experimental set-up for the vessel current (VC) measurement. One probe consists of two insulated wires connected for the observation ports. Wires are connected with the external resistance of 100 Ω which is sufficiently large in comparison with the impedance between the observation ports. Two probes are installed on each port section, one measures the voltage between top- and equatorial-port, and another one measures the voltage between bottom- and equatorial-port. Such a measurement was carried out in RFX [5], and the voltage probes were installed on three toroidal sections. In our experiments, the voltage probes are installed on 15 toroidal sections, and the relation between the position of the Locked mode and the VC is examined more well-informed. The observed signal contains not only the voltage drop due to the VC flowing but also the toroidal flux swing variation. The wire is located at the outside of the thick shell, and the vacuum vessel and the wire form a flux loop which can sense the toroidal flux variation as shown in figure 1. The analysis for the experimental results was carried out considering fol-

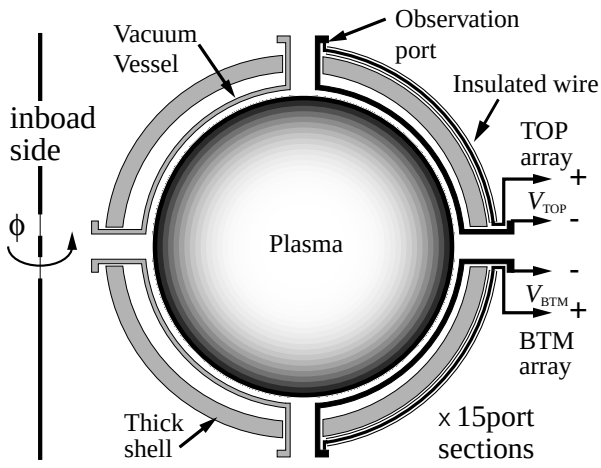

Figure 1: Experimental set-up for the vessel current measurement. Two voltage probes are installed on each poloidal plane.

lowing fact in order to extract the value of the VC.

(A) The inductance of the load can not be neglected, and it is estimated at L_{load} = 0.32 μH. Here, it is assumed that the current flows in the poloidal direction, and that the load is one-4th of the single turn coil which is one-16th that of the vacuum vessel. We also obtain the resistance of the load, R_{load} = 0.12 mΩ. The vessel current $I(t)$ is expressed by the following equation,

$$L_{load}\, dI(t)/dt + R_{load}\, I(t) = F(t), \quad (1)$$

where $F(t)$ is the measured voltage.

(B) In order to extract VC out of the effects of the toroidal flux variation and the error in the measurements (e.g. the location of the probe and wire), we use a reference shot, in which Δ_T is smallest in each discharge conditions. We subtract the VC of the reference shot $I_{reference}(t)$ from $I(t)$.

$$I^*(t) = I(t) - I_{reference}(t). \quad (2)$$

(C) In order to understand underlying physics of the experimental results, we evaluate the sum (counter component) and difference (net component) of $I^*_{top}(t)$ and $I^*_{btm}(t)$, and obtain

$$I^*_{counter}(t) = I^*_{top}(t) + I^*_{btm}(t) \text{ and } I^*_{net}(t) = I^*_{top}(t) - I^*_{btm}(t). \quad (3)$$

(D) In order to estimate the toroidal fluctuation of $I^*(t)$, the toroidal average of $I^*(t)$, $\langle I^*(t)\rangle_{toro}$ is subtracted,

$$\Delta I^*_{counter}(t) = I^*_{counter}(t) - \langle I^*_{counter}(t)\rangle_{toro} \text{ and } \Delta I^*_{net}(t) = I^*_{net}(t) - \langle I^*_{net}(t)\rangle_{toro}. \quad (4)$$

This is to emphasize the relative change of the VC along the toroidal direction.

Figure 2 shows the ensemble average of Δ_T, $\Delta I^*_{counter}$, and ΔI^*_{net} at t = 20ms for the 31 shots in the experimental condition which the Locked mode exists almost in every discharge. Here after, $\langle X\rangle_e$ means the ensemble average of the quantity of X. The position where Δ_T becomes a maximum value is defined as the locked position, and the locked position is made to be 0 degree of the toroidal angle. $\Delta I^*_{counter}$ has a peak near the locked position. On the other hand, the correlation between the locked position and ΔI^*_{net} is not clearly seen.

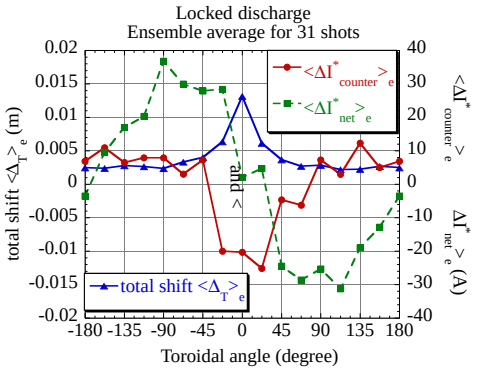

Figure 2: the ensemble average of Δ_T, $\Delta I^*_{counter}$, and ΔI^*_{net} at t = 20ms for the 31 shots.

3. Discussions

The possible causes of the Locked mode, the existence of the halo current and the breaking effect of the eddy current in the vacuum vessel on the mode rotation, are discussed here.

3.1 The existence of the halo current.

For the poloidal current can be induced by the toroidal flux swing, and the direction of the induced current is the same as the current in the toroidal field coil (TFC) in reversal phase. The induced current in the plasma periphery is pulled by the electromagnetic force for the TFC, and flows into the vacuum vessel. 'Halo current' is used with the meaning that part of the plasma current flows in the external conducting structure and returns to the plasma. The driving voltage for the poloidal current, $|V_\theta| = d\Phi/dt$, is estimated at 2 V (=0.04 Wb / 20 ms) during the current rising phase (Figure 3). When the width of the current channel in the vacuum vessel in the

toroidal direction is assumed to be one 16th of the torus, the resistance of the current channel is four times the R_{load} (~ 4 x 0.12 mΩ) and the current is estimated to be 4.0 kA.

The cross correlation between $<\Delta_T>_e$ and $<\Delta I^*_{counter}>_e$ at t = 20 ms, shows that there is the correlation for the locked position and the position where $\Delta I^*_{counter}$ become a maximum, though it seems that the position of maximum $<\Delta I^*_{counter}>_e$ is slightly shifted from the locked position (figure 4 a)). It can be seen that there is a correlation between $\Delta I^*_{counter}$ and the locked position, because such a correlation is not seen in the experimental condition where LM does not exist almost in every discharge (figure 4 b)). In spite of the correlation, we conclude that $\Delta I^*_{counter}$ is not the halo current. The halo current always flows in a fixed poloidal direction. The cross correlation between $<\Delta_T>_e$ and $<\Delta I^*_{net}>_e$ should appear clearly than the cross correlation between $<\Delta_T>_e$ and $<\Delta I^*_{counter}>_e$, if the VC flows in a fixed poloidal direction. The experimental result does not agree with this. Namely, significant amount of the net poloidal vessel current does not flow at the locked position. In addition, the experimental results of the toroidal variation of the VC (order of 20 A) is much less than the expected value (order of kA). These results indicate that the halo current may not be the cause of the locked mode existence.

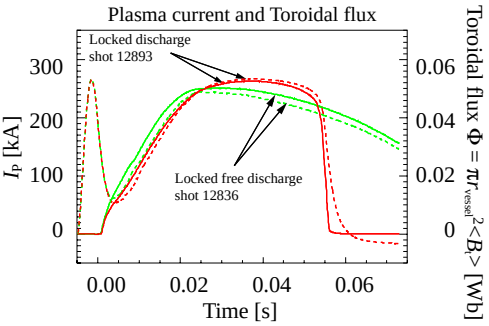

Figure 3: Plasma current and toroidal flux.

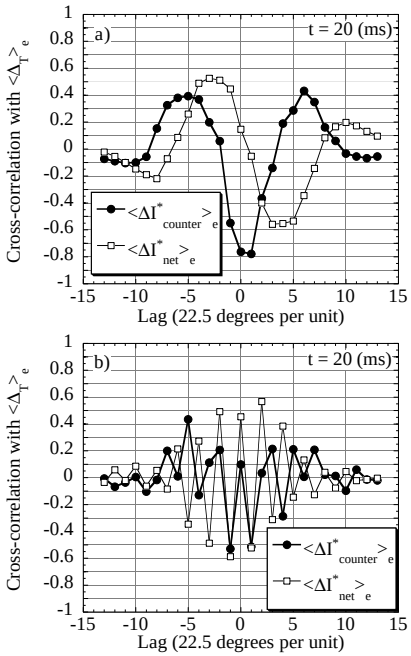

Figure 4: Cross correlation with $<\Delta_T>_e$ for the locked discharges (a) and for the locked-free discharges (b).

3.2 The breaking effect of the eddy current in the vacuum vessel on the mode rotation.

Figure 5 shows the mode amplitudes of the radial magnetic fluctuation (left), δB_r, the mode amplitudes of the toroidal magnetic fluctuation (center), δB_T and the totoidal angular phase velocities of δB_T (right). Dominant modes (n=6, 7, and 8) of m=1 are plotted. Red lines show the ensemble averaged value for the locked discharges (total 31 shots), and green lines show the ensemble averaged value for the locked-free discharges (total 20 shots). The amplitude of δB_T grows during the current rising phase (t < 0.02 s) in the locked discharge. After 0.02 s, the mode (n=6) amplitudes of δB_r and δB_T tend to be same in both conditions, but the total amplitudes are larger in locked discharge than in locked-free discharge. δB_T are observed to rotate in both condition before 0.02 s, and the mode rotation stop after 0.02 s.

In Fitzpatrick's theory [4], when $n\Omega_{s0}\tau_b$ is less than $b/\delta b$, the vessel is considered as the thin shell. When $n\Omega_{s0}\tau_b$ is greater than $b/\delta b$, the vessel is considered as the thick shell. Here, $n\Omega_{s0}$ is the angular phase velocity of typical dynamo modes without the breaking effect, τ_b is the time constant of the vessel, b is the radius of the vessel, δb is the thickness of the vessel. The $n\Omega_{s0}$ is given as following, $n\Omega_{s0} \sim 6T_{e0}/(a^2B_0) = (12\pi/a\mu_0)(T_{e0}/I_p)$. Here, a is the minor radius of the

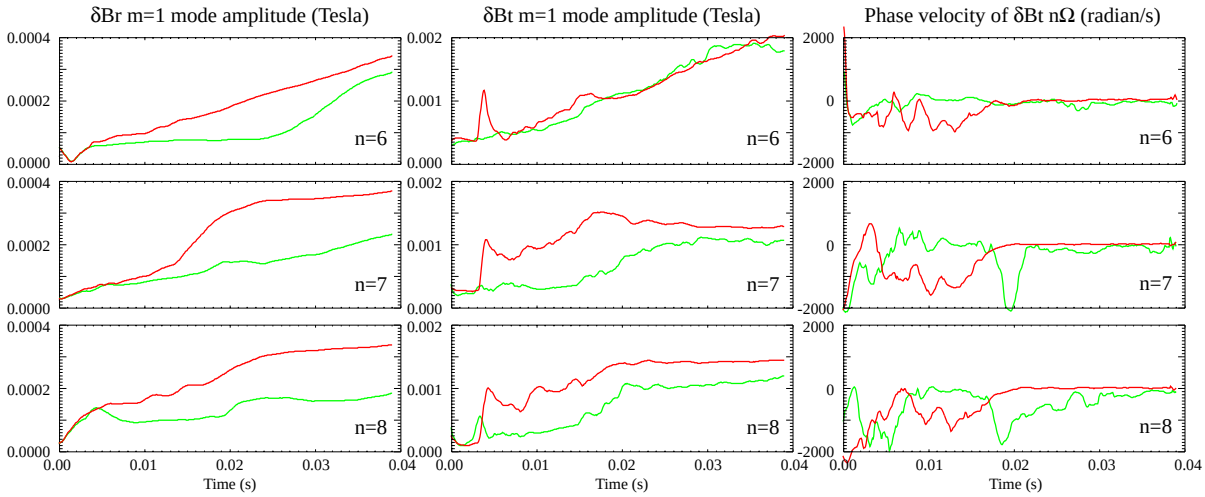

Figure 5: Ensemble averaged mode amplitudes of δB_r (left), δB_T (center), and phase velocities of δB_T (right) for the locked discharges (red lines) and for the locked-free discharges (green lines).

plasma, and T_{e0} is the plasma electron temperature. The critical value of radial magnetic field at the rational surface, $b_s^{m,n}$ is proportional for $(n_{e0}/\tau_E)^{1/2}(T_{e0}/I_p)$ in the thin shell approximation, and it is proportional for $(n_{e0}/\tau_E)^{1/2}(T_{e0}/I_p)^{3/4}$ in the thick shell approximation. Here, τ_E is the energy confinement time, and n_{e0} is the plasma electron density. It is assumed that the various equilibrium plasma profiles remain constant. Figure 6 shows the plasma electron temperature measured by Thomson-scattering. The peak value of T_{e0} is almost the same for both conditions. However, T_{e0} is higher in locked-free discharge than locked discharge before 0.02 s. I_p is almost the same in both condition as shown in figure 3. Since τ_E, β_p and $n_{e0}T_{e0}$ is almost same in the both conditions, $b_s^{m,n}$ depend on $T_{e0}^{1/2}$ in thin shell approximation and on $T_{e0}^{1/4}$ in thick shell approximation. It follows that $b_s^{m,n}$ and $n\Omega_{s0}$ are smaller in the locked discharge than the those in the locked-free discharge. Thus, the plasma electron temperature is one of the key parameter of the locked mode existence.

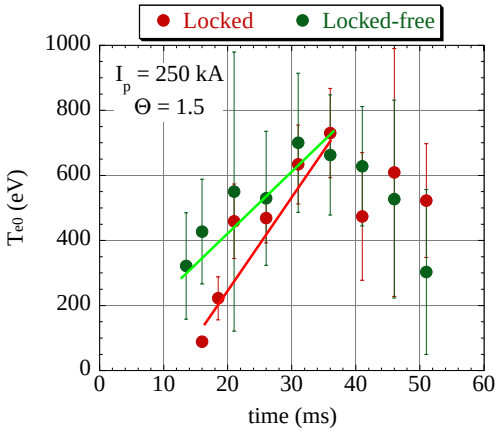

Figure 6: Plasma electron temperature measured by Thomson-scattering, T_{e0} for the locked discharges (red circle) and for the locked-free discharges (green circle).

4. Conclusions

The vessel current measurement shows that the halo current may not be the cause of the locked mode. The temporal behavior of the magnetic fluctuations and of the electron temperature indicate that the braking effect of the eddy current [4] is a cause of the locked mode existence.

References [1] Almagri A F *et al* 1992 *Phys. Fluids* **B4** 4080. [2] Buffa A *et al* 1994 *Proc. of 21st EPS Conf. on Control. Fusion and Plasma Phys. Montpellier,* European Physical Society, Petit-Lancy, part I, p 458. [3] Yagi Y *et al* 1999 *Phys. Plasmas* **6** 3824. [4] Fitzpatrick R *et al* 1999 *Phys. Plasmas* **6** 3878. [5] Peruzzo S et al 1997 *Proc. of 24th EPS Conf. on Contorol. Fusion and Plasma Phys., Berchtesgaarden.*